Energy Proceedings
Vol 38, 2024
ISSN 2004-2965

Vehicle-to-X Service Provision for various Modes of e-Transportation with Consideration of the Influence on Lithium-Ion Battery Utilization

Benedikt Tepe[1*], Sammy Jablonski[1], Anupam Parlikar[1], Holger Hesse[2], Andreas Jossen[1]

1 Technical University of Munich (TUM), School of Engineering and Design, Department of Energy and Process Engineering, Chair of Electrical Energy Storage Technology, Germany

2 Kempten University of Applied Sciences, Department of Mechanical Engineering, Institute for Energy and Propulsion Technologies, Germany

(*Corresponding Author: benedikt.tepe@tum.de)

ABSTRACT

The electrification of transportation modes such as cars, buses, and boats offers the potential of providing vehicle-to-X services during idle times. Pools of vehicles can provide balancing power, trade on the electricity market, or be used for load peak shaving. In this work, the usage patterns of electric cars, electric buses, and electric boats are investigated, and the provision of vehicle-to-X with these vehicles is simulated using an open-source simulation tool. A data analysis and a vehicle usage pattern assessment show that especially private electric cars behave predictably at night. It also reveals that the vehicle-to-X availability varies over the week for all vehicle types and is highest at night for cars and buses. During the day on weekdays, private cars are available for vehicle-to-X 30 to 70% of the time, the analyzed buses 5 to 50% of the time, and the availability of the boats depends on their primary use as ferries or private boats. If the three transportation modes provide vehicle-to-X during idle times, the equivalent full cycles that the lithium-ion batteries complete increase at different rates depending on the vehicle pool size, while the mean charging rates decrease. Furthermore, an exemplary aging analysis shows that the additional load of vehicle-to-X provision slightly increases the capacity loss of the car batteries compared to a paused unidirectional charging strategy.

Keywords: electric vehicles, vehicle-to-X, vehicle-to-grid, lithium-ion batteries, transportation means, battery degradation

NOMENCLATURE

Abbreviations

BSS	Battery storage system
e-Boat	Electric boat
e-Bus	Electric bus
e-Car	Electric car
EFC	Equivalent full cycle
FCR	Frequency containment reserve
LFP	Lithium iron phosphate
LIB	Lithium-ion battery
PS	Peak shaving
SOC	State of charge
V2B	Vehicle-to-building
V2G	Vehicle-to-grid
V2H	Vehicle-to-home
V2X	Vehicle-to-X

Parameters and Symbols

b(t)	Binary value indicating connection to electricity grid
j	Current timestep in period
m	Number of periods
n	Number of timesteps in period
P(t)	Power
$Pred_j$	Predictability score at current timestep
v(t)	Binary value of current V2X-ready ratio

This is a paper for 15th International Conference on Applied Energy (ICAE2023), Dec. 3-7, 2023, Doha, Qatar.

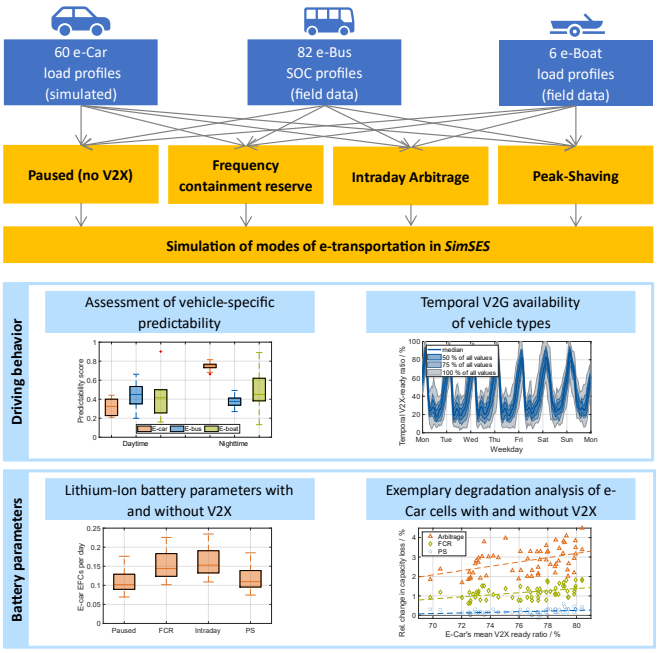

Fig. 1. Graphical overview. Three vehicle types and four charging strategies are simulated with *SimSES* to generate results on driving behavior and battery-relevant

1. INTRODUCTION

The electrification of vehicles plays an essential role in decarbonization [1]. This is one of the reasons why the number of electric cars (e-Cars), electric buses (e-Buses), and electric boats (e-Boats) increase worldwide [1–3]. These vehicles introduce relatively large storage capacities to the market through their batteries [4]. From an economic perspective, it is therefore essential to exploit the potential of vehicle batteries during idle times. When the vehicles are connected to the electricity grid, they can be used for various purposes in the future [5]: First, they can contribute behind-the-meter to consumption of photovoltaic energy via vehicle-to-home (V2H), as is done with stationary home battery storage systems (BSS) [6]. Another behind-the-meter application is peak-shaving (PS), where pools of vehicles help meet peak loads in vehicle-to-building (V2B) [6]. Second, the vehicles can participate in electricity trading or provide grid services using vehicle-to-grid (V2G), corresponding to front-the-meter applications [7,8]. For example, arbitrage trading is performed on the intraday market in the former. In the latter, pools of vehicles can provide, for example, frequency containment reserve (FCR) to compensate for frequency fluctuations in the electricity grid. Generally, the bidirectional use of electric vehicles during idle times is called vehicle-to-x (V2X) [5].

Using vehicles in V2X can generate additional revenue and bring environmental benefits by increasing battery utilization. However, it also leads to a higher load on the vehicle batteries. With suboptimal planning, the provision of V2G can increase the degradation of vehicle batteries [9]. An increased degradation of vehicle batteries when providing primary frequency regulation was also shown by Thingvad et al. in a field trial in Denmark [10].

A detailed evaluation of the impact of V2X on various battery-related parameters is part of this work. Open-access data from previous publications is used to simulate the provision of V2X in the storage simulation tool *SimSES* [11] (section 2 and section 3). The focus is on the applications FCR, intraday arbitrage trading, and PS. We use driving profiles of simulated private e-Cars and field data of city e-Buses and e-Boats. This way, various vehicle types and V2X applications are combined and analyzed. The key contributions include an analysis of the predictability of the vehicles (section 4.1), an analysis of the V2X availability of the vehicle types (section 4.2), an evaluation of the influence of V2X provision on battery-relevant parameters (section 4.3), and an exemplary degradation analysis of the e-Car batteries (section 4.4).

The innovative points of this work are enabling the simulation of V2X services in the open-source tool *SimSES*, statements on the V2X capability of various vehicle types, and the impact of V2X deployment on battery-relevant parameters.

2. DATABASE

2.1 Data of mobile BSS applications

Due to the growing electrification of vehicles, such as buses, cars, and boats, lithium-ion batteries (LIBs) are increasingly being installed in these means of transport as traction batteries. For the simulation of the three means of transportation, we rely on data published as open data in a previous work [12,13]. Based on this work, load profiles of 60 e-Cars and six e-Boats and state-of-charge (SOC) profiles of 52 e-Buses are available (see Table 1). The profiles have varying lengths, and the simulations in this work are always performed over the entire length of a vehicle profile.

2.2 Data of stationary BSS applications

Stationary BSSs are used in various applications. For example, they can perform arbitrage trading on the electricity market or provide grid services like FCR. Parked electric vehicles can also participate in these markets if they are connected to the electricity grid and

Table 1: Data on the transportation means and the stationary BSSs used for V2X provision.

Data	# of datasets	Data length	Reference
e-Cars	60	One year	Tepe et al. [13] based on Gaete-Morales et al. [16]
e-Buses	52	3 to 14 months	Tepe et al. [13]
e-Boats	6	3 to 9 months	Tepe et al. [13]
FCR	1	One year	Kucevic et al. [14]
PS	1	One year	Kucevic et al. [14]
Arbitrage	1	One year	Collath et al. [15]

combined in pools. In the following sections these applications are called V2X applications. To simulate the V2X applications in *SimSES*, we use storage load profiles that we defined in a previous work as representative load profiles for the PS and FCR applications [14]. Since the PS profile was developed with a storage system with a maximum power of 40 kW and the vehicles' charging and discharging power range from 11 to 150 kW, the PS profile was scaled up by a factor of 10 so that its maximum power now corresponds to 400 kW. For the arbitrage application, we use a load profile determined in a research work by Collath et al., who optimized arbitrage trading with a stationary BSS considering calendar and cyclic degradation [15].

3. METHODOLOGY AND SIMULATION FRAMEWORK

3.1 SimSES: Simulation of EVs and V2X provision

The open-access storage system simulation tool *SimSES* was developed at the Technical University of Munich and has been presented in detail in a previous publication [17]. In our work on e-transportation and their utilization of batteries, the extension of *SimSES* to mobile applications was explained [12]. The publication compared charging strategies such as uncontrolled charging versus paused charging, where charging was performed after arrival to a minimum SOC and paused until just before departure. This paused strategy was extended for this work to allow vehicles to provide V2X during the paused period. This is done by superposing a V2X load profile of one of the stationary applications FCR, PS, or arbitrage over to the load (e-Cars, e-Boats) or SOC (e-Buses) profile. As soon as the respective vehicle is at home (e-Car), in the depot (e-Bus) or at the dock (e-Boat), it is charged to a minimum SOC of 50%. Subsequently, the provision of V2X is simulated until the time when charging is required again for the vehicle to be fully charged at departure. The e-Buses are charged to the departure SOCs logged in real operation, as described in a previous publication [12]. Alternative approaches of charging strategies, for example charging only the amount of energy needed for the next trip, are not part of this work. For the estimation of the departure time, perfect foresight is assumed. To calculate the required V2X power at every point in time, the power of the V2X profile is divided by the number of currently existing vehicles in the pool and assumed to be the power to be provided by the vehicle. This means each vehicle in the pool must provide the same fraction of the total pool power. The estimation of the available number of vehicles is explained in section 4.3, as this is based on results from section 4.2. During V2X operation, the SOC of the vehicle can drop below 30%. If this is the case, the V2X operation is paused, and the vehicle is recharged to 50% so that at least 30% is always available for spontaneous trips. In a field test, users have reported an average of 34% as the minimum desired available SOC [18].

This work uses batch simulations to simulate the 60 e-Cars, 52 e-Buses, and six e-Boats in the three V2X markets FCR, arbitrage trading, and PS. *SimSES* then determines a variety of metrics that are calculated for each vehicle with each V2X market. One metric of *SimSES* is the binary quantification of whether the vehicle can be used for V2X at a point in time. The calculation of this value is shown in equation (1). This is the case when the e-Car is at home, the e-Bus at the depot, and the e-Boat at the dock ($b(t) = 1$) and not being charged ($P(t) = 0$). If the condition is met, the plugged-and-idle value $v(t)$ is 1. In contrast, if the vehicle is on the road or currently charging the plugged-and-idle value is 0. The proportion of the total time the vehicle can be used for V2G was referred to as the temporal V2G-ready ratio in [12]. Analogously, the value in this work is called V2X-ready ratio to imply that V2H and V2B could also be provided.

$$v(t) = \begin{cases} 1, & P(t) = 0 \; and \; b(t) = 1 \\ 0, & otherwise \end{cases} \quad (1)$$

3.2 Quantification of driving behavior predictability

The suitability of vehicles for V2X depends on various factors. These are, for example, the driving behavior, the grid connection times, and the predictability of departures and arrivals. For electric vehicle aggregators, it is relevant to be able to predict or estimate the available pool size at any given time. Supposing that the vehicle owner does not provide the next departure or arrival time, or it cannot be determined from bus

schedules, historical data can be used to estimate when the vehicle will depart. However, for historical data, estimating the extent to which the vehicle is used according to repetitive behavior, such as a daily commute or a trip to a weekly recreational activity, is crucial. The predictability is to be quantified as explained in the next paragraph.

For the investigation of the weekly periodicity, the respective $v(t)$ vector is first decomposed into weekly segments. Figure 2 a) shows $v(t)$ for an exemplary e-Car for each hour of the week over the year. The hourly resolution is chosen here for a better visualization and results from the mean value of the 60 one-minute values. This results in values between 0 and 1 in addition to the binary values. Moreover, Figure 2 b) indicates the probability that the value for $v(t)$ is 1 at a certain time during the week. At times when the probability is close

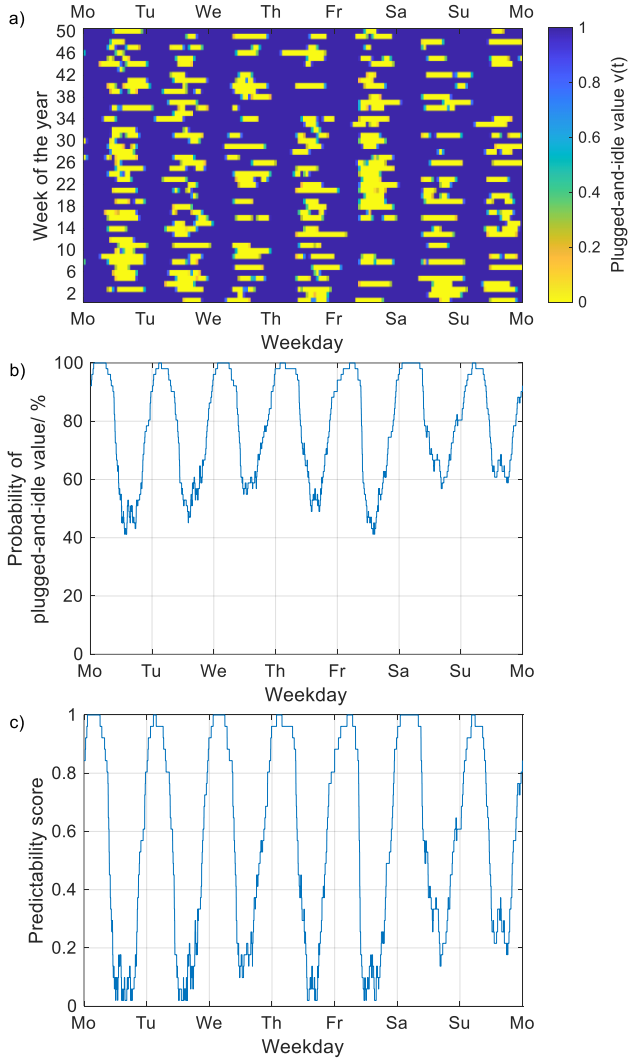

Fig. 2. Hourly plugged-and-idle values of one exemplary e-Car over the year segmented in weeks (a), probability of plugged-and-idle values of one over the week (b), and predictability score over the week (c).

to 100%, the vehicle can be used frequently for V2X. The diagrams show that there are phases during the week when the vehicle could provide V2X relatively consistently, such as Wednesday nights. Likewise, there are phases when the vehicle is often not available for V2X, such as Monday afternoons. For aggregators, these consistent phases are desirable because the vehicle is predictable. Less desirable are phases in which the vehicle is sometimes available and sometimes on the road. The worst case from the aggregator's point of view is when the vehicle is, on average, 50% available at one point in time. On the other hand, average values of 0 and 100% are desirable because the vehicle is fully predictable during these times. We now determine a predictability score at each point of time of the week using equation (2). Therefore, we subtract 0.5 from the mean value of the values at one point in the week and multiply the absolute value by two. If the mean value is 0.1, for example, this results in a predictability score ($Pred$) of 0.8. The same $Pred$ results from a mean value of 0.9. In contrast, the worst case mean value of 0.5 leads to a $Pred$ of 0.

In addition to the weekly period shown here, periods of 24 hours or 30 days, for example, can also be used. No distinction would be made between working days and weekend days in the case of daily periods. If monthly periods were used, events occurring monthly could be better captured and predicted.

$$Pred_j = \left| \frac{\sum_{k=1}^{m} v_j^k}{m} - 0.5 \right| \times 2 \qquad (2)$$

With:

$$\boldsymbol{v} = \begin{bmatrix} v_1^1 & v_1^2 & \dots & v_1^m \\ v_2^1 & v_2^2 & \cdots & v_2^m \\ \vdots & \vdots & \ddots & \vdots \\ v_n^1 & v_n^2 & \cdots & v_n^m \end{bmatrix}$$

m: $Number\ of\ periods$

n: $Number\ of\ timesteps\ per\ period$

$$\overrightarrow{Pred} = \begin{bmatrix} Pred_1 \\ Pred_2 \\ \vdots \\ Pred_n \end{bmatrix}$$

$Pred_j \in \{0; 1\} \quad j = 1 \dots n$

3.3 Lithium-ion battery relevant KPIs and effects on battery degradation

LiBs are subject to degradation effects, which can be separated into calendar and cyclic aging [19]. While the former occurs permanently over time, the latter depends on the cyclization of the battery. Various parameters

influence the degradation of LIBs so that the utilization of LIBs can be quantified with respect to those parameters [12]. For example, the equivalent full cycles (EFCs) can be measured and compared with each other in various applications. For this purpose, the energy throughput is divided by the nominal energy of the battery. In general, higher cyclization, an increase in EFCs, leads to accelerated cyclic degradation. However, the extent of the increased degradation differs for different cell chemistries, as there exist more cycle-stable and less cycle-stable chemistries [20]. Another relevant parameter is the average SOC experienced by the LIB. For example, if private e-Cars are charged immediately after arriving at home, the mean SOC is relatively high because the vehicles are parked for a long time at high SOCs [12]. If, in contrast, charging takes place later or with a pause, the mean SOC of the battery can be reduced [12]. The mean SOC also influences the degradation of LIBs [19]. For most LIBs, high mean SOCs should be avoided because an accelerated solid electrolyte interphase growth occurs in those SOC ranges [20]. This effect amplifies the calendar degradation of the LIB. The last parameter calculated in this work is the charging rate (C-rate), which describes the current at which a battery is charged or discharged in relation to the nominal capacity of the battery [12]. The C-rate also influences cyclic degradation. If LIBs are exposed to comparatively high C-rates, cyclic degradation increases [19]. In addition, other factors play a role in degradation, such as temperature and depth of discharge [20]. The decrease of remaining capacity and the increase in resistance of a LIB then result from an interplay of the various influencing factors. In *SimSES*, for example, semi-empirical aging models are implemented for a Sony lithium iron phosphate (LFP) cell, published by Naumann et al. [21,22], and a nickel manganese cobalt (NMC) cell, published by Schmalstieg et al. [23]. Since many e-Buses and an increasing number of e-Cars have LFP batteries installed [1,24], we use the LFP model in section 4.4, which relies on a half-cycle counter.

4. RESULTS

This section presents the results of the work. First, the vehicle-specific predictability is analyzed in section 4.1. Afterwards, the V2X-ready ratio of the three vehicle types is illustrated in detail in section 4.2. Then, in section 4.3, battery-relevant parameters for V2X-providing vehicles are compared with those of unidirectional charged vehicles. Finally, in section 4.4, the influence of V2X provision on battery aging is shown using an exemplary LFP cell for the e-Cars.

4.1 Assessment of vehicle-specific predictability

The following section quantifies the driving behavior predictability of the vehicles according to the calculation from section 3.2. The presented analysis was performed for each vehicle to determine the course of the predictability score. The mean predictability scores for all vehicles are shown as boxplots in Figure 3. The periods used for the predictability scores are 24 hours (a) and seven days (b), as shown in Figure 2. Due to the significant differences in predictability scores between daytime and nighttime, Figureshows the results for daytime (left) and for nighttime (right). The results for the three vehicle types are displayed and derived from the mean predictability scores of the 60 e-Cars, 52 e-Buses, and six e-Boats.

For the e-Cars, high predictability scores of 0.66 to 0.82 are achieved at night. Here, the simulated e-Cars behave relatively predictably. The e-Buses show smaller differences among themselves at night than during the day, where the scores are between 0.27 and 0.7 for the weekly pattern, for example (Figure 3 b)). At the same time, however, the median score of the buses at night is lower than the median score of the daytime. This can be explained by the fact that the required charging energy at night depends on the driving distance during the prior day, and thus the e-Buses are irregularly available for V2X at night while they are mostly on the road during the day. The e-Boats show large scatter in their predictability scores both during the day and at night. For example,

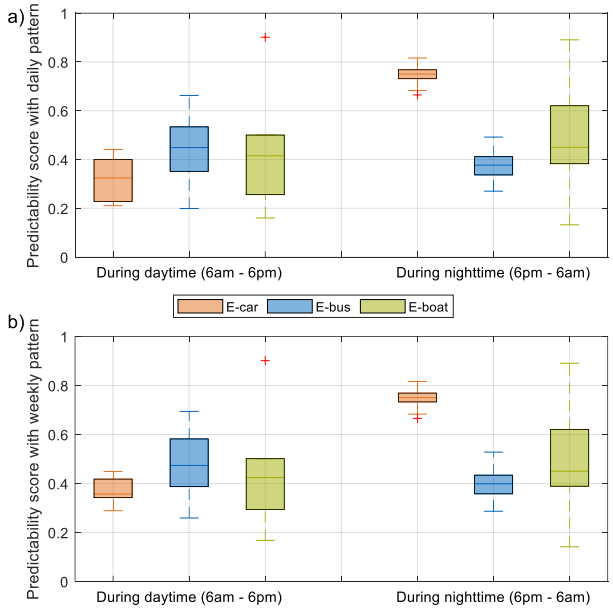

Fig. 3. Average predictability score of every vehicle during daytime (left) and during nighttime (right) using the predictability forecast for daily pattern (a) and weekly pattern (b).

there is one boat that achieves scores above 0.8. At the same time, there is another boat whose scores are below 0.2. Depending on the use of the boats as a ferry or pleasure vessel, the predictability therefore differs. Lastly, the usage of the daily pattern (Figure 3 a)) can be compared to that of the weekly pattern (Figure 3 b)). Especially for the e-Cars with their varying driving behavior between weekdays and weekends, the predictability scores increase when using a weekly pattern especially during the day. Moreover, the range of the results decreases for the e-Cars using the weekly pattern. The e-Buses also show slight improvements in predictability scores for daytime hours when changing from daily to weekly pattern and no changes at night. In contrast, no differences are observed for the e-Boats.

4.2 Temporal V2X availability of vehicle types

The V2X-ready ratio indicates the proportion of the time a vehicle can be used for V2X, as explained in section 3.1. For the e-Cars, for example, we found mean temporal V2X-ready ratios (respectively V2G-ready ratios) of 70 to 80% in a previous work [12]. At this point, the V2X-ready ratios are analyzed in more detail. Figure 4 shows the V2X-ready ratio of the three modes of transportation over a week. The dark line shows the median and the shading indicates the distributions with 50%, 75%, and 100% of all values. A value of 33% on Monday at noon means that the vehicle would be available for V2X on average every third Monday at noon. A value of 67% indicates that the vehicle would be available two out of three Monday noon times.

The private e-Cars show high temporal V2X-ready ratios of 90 to 100% at night (Figure 3 a)). On weekdays, the ratio drops to 30 to 70%, depending on the commuting behavior of the vehicle. On weekends, the ratio is also higher during the day, with 50 to 80%. E-Buses also have the highest V2X-ready ratio at night, with 50 to 100% (Figure 3 b)), although this is below the ratio of the e-Cars. During the day, the ratio drops to 5 to 50%, as the e-Buses are mostly on the road. The daytime behavior does not change much on weekends compared to weekdays. The e-Boat results are divided into two groups (Figure 4 c)): High-utilization e-Boats and low-utilization e-Boats. The high-utilization e-Boats have temporal V2X-ready ratios of mostly below 40%. The low-utilization e-Boats, in contrast, have ratios between 30 and 90%. Therefore, the e-Boats' potential differs greatly depending on how they are used. Moreover, the e-Boats do not show a typical daily pattern compared to the e-Cars and e-Buses. This is because the e-Boats are often charged at low power in the dock. In addition, low-

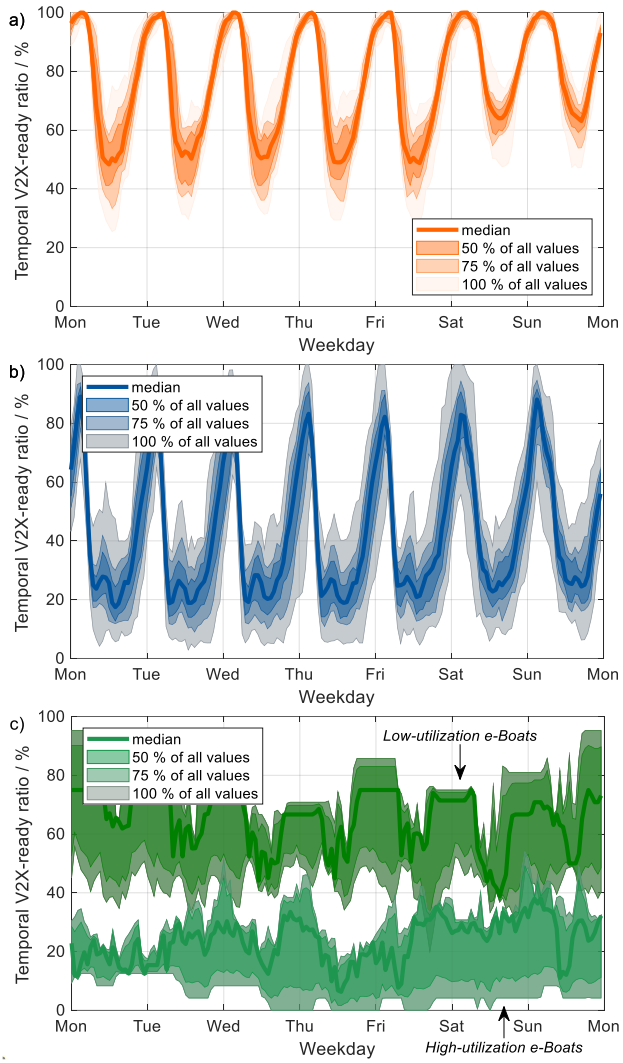

Fig. 4. Temporal V2X-ready ratio over the week using an uncontrolled charging strategy for the e-Cars (a), e-Buses (b), and e-Boats (c).

utilization e-Boats, for example, usually remain unused in the dock during the day as well as at night, resulting in no day-night rhythm as with the e-Buses and e-Cars. Overall, the evaluation shows that the temporal V2X potential of the vehicles varies over a week. Especially at night, e-Cars and e-Buses can be used for V2X. For e-Boats, the potential depends on the use of the boats.

4.3 Lithium-ion battery parameters with and without V2X

The provision of V2X changes the load on vehicle batteries. The extent of this change is examined in this section. Battery-relevant parameters considered in this work are the number of EFCs, the mean SOC, and the mean C-rates. The simulations are performed with *SimSES,* as described in section 3.1. Since the stationary applications FCR, PS, and arbitrage were generated for one large stationary BSS, the individual vehicles in the

Table 2: Pool size calculations. For determining the pool size, the maximum power required for V2X is divided by the maximum charging power (which equals the maximum discharging power) of the vehicles and by the assumed minimal temporal V2X-ready ratio.

Transportation means	e-Car			e-Bus			e-Boat		
Min. considered temporal V2X-ready ratio	40%	40%	40%	10%	10%	10%	10%	10%	10%
Max. charging power	11 kW	11 kW	11 kW	150 kW	150 kW	150 kW	11 kW	11 kW	11 kW
V2X market	FCR	Intraday	PS	FCR	Intraday	PS	FCR	Intraday	PS
Max. V2X power	1.2 MW	1 MW	400 kW	1.2 MW	1 MW	400 kW	1.2 MW	1 MW	400 kW
Required EVs in pool	273	228	91	80	67	27	1091	910	364

pool of vehicles only need to provide a fraction of the power of the original stationary storage. In general, the respective fractions depend on the current pool size. In previous works, we determined economically optimal pool sizes for commercial e-Cars to generate as much revenue as possible with as few vehicles as possible [7,25].

In this work, we estimate the total pool sizes based on the temporal V2X-ready ratio and the maximum power of the vehicle batteries and charging stations (see Table 2). For example, for the provision of FCR, a pool of 80 e-Buses is required to be able to deliver the 1.2 MW of maximum power at a minimal temporal V2X-ready ratio of 10%. The worst-case temporal V2X-ready ratio of the buses is 3% (Tuesday afternoon), according to Figure 4 b). Dimensioning the pool to this availability would significantly oversize the pool. Aggregators would likely switch to stationary backup BSS rather than sizing the pool for the annual minimum. As shown in Figure 4 b), the assumed 80 buses are not permanently available. The median temporal V2X-ready ratio fluctuates between 17% and 89% over the week. For this reason, the available number of vehicles is determined from the median temporal V2X-ready ratio at each point in time of the simulation, depending on the time of the current week. If the ratio is 17%, only 14 buses are available for FCR. If, on the other hand, the ratio is 89%, 71 buses are available. The V2X power to be provided at any given time is then divided among the currently available vehicles.

The simulation results for the three parameters daily EFCs, mean SOC and mean C-rate are shown in Figure 5. The subfigures are divided into e-Cars (left), e-Buses (center), and e-Boats (right). For each vehicle category, the boxplots of the three V2X markets are compared to the unidirectional paused charging strategy without V2X. Likewise, a comparison with an uncontrolled strategy would be possible [12]. At this point, however, we want to compare paused charging with the V2X-providing charging strategies.

Figure 5 a) shows the daily EFCs of the 60 e-Cars as boxplots once for the paused charging strategy and once for the three V2X markets. The e-Cars encounter 0.07 to 0.18 EFCs per day in the paused charging strategy. In contrast, in the FCR and intraday arbitrage applications, the number of daily EFCs increases to a range of 0.1 to 0.23. For the median values, this corresponds to an increase of 42 to 50%. The provision of PS increases the median daily EFCs by only 8%. With unidirectional charging, the e-Buses encounter more cycles than the e-Cars due to the longer driving distances (see Figure 5 b)). As a result, the e-Buses are available for V2X less often than the e-Cars (see Figure 3). Consequently, the daily EFCs of the e-Buses increase only slightly with the additional provision of V2X. The median FCR and intraday EFCs are 7 to 13% higher than those of paused charging strategy. If PS is provided, the median daily EFCs increase by only 1%. This is because in PS operation, the BSS capacity is rarely used. The stationary BSS used to generate the PS profile performed 21 EFCs over one year, while the FCR providing BSS completed 270 EFCs [14]. The e-Boats perform 0.026 to 0.277 EFCs daily with paused charging (see Figure 5 c). This means that the least used boat makes one EFC every month, and the most used boat makes one EFC every 3.6 days. If the e-Boats are now used for FCR during idle periods, the daily EFCs increase by 1% to 40%. Similar values result in intraday trading. Accordingly, EFCs increase when e-Boats are frequently used for V2X. However, if a boat is rarely available, the number of EFCs increases only slightly. The results for PS are similar to those for e-Cars and e-Buses.

The mean SOCs of vehicle batteries are also affected by the provision of V2X (Figure 5 d) - f)). Compared to the paused unidirectional charging strategy, the mean SOCs change slightly as the V2X provision charges and discharges the batteries. The median mean SOC of the e-

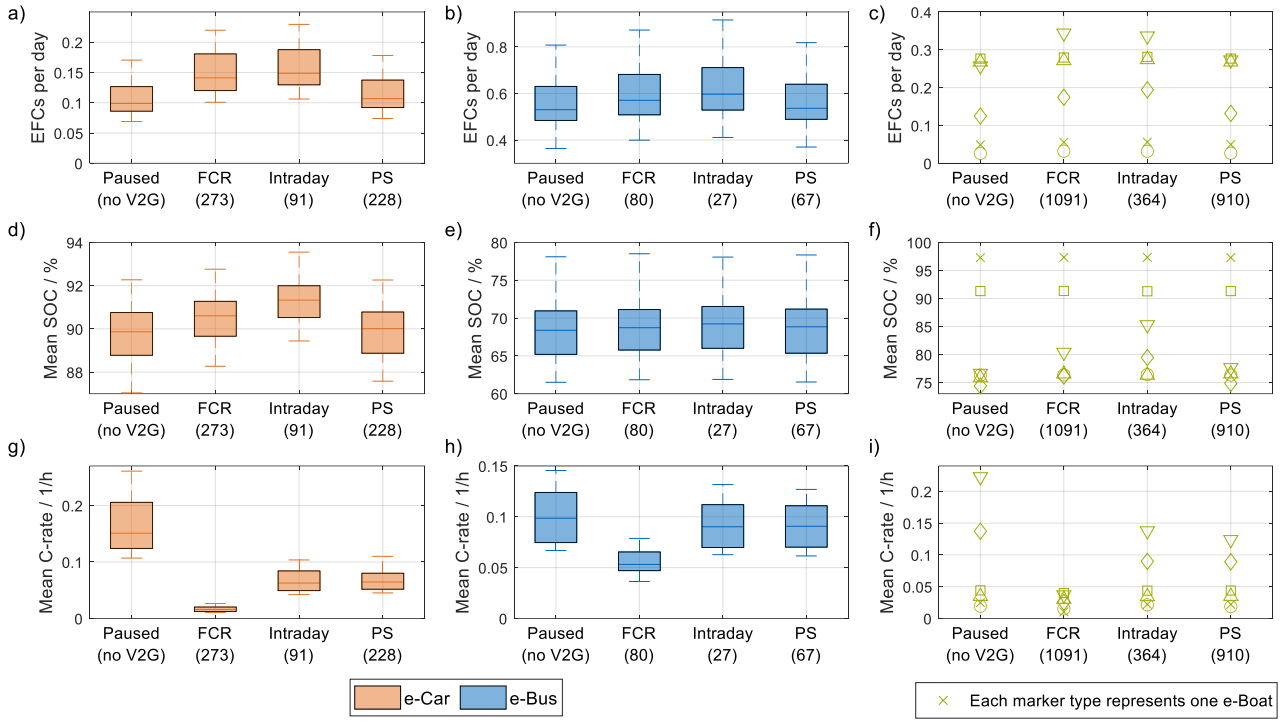

Fig. 5. Battery-related parameters of the e-Cars, e-Buses, and e-Boats. (a) EFCs per day, (b) mean SOC, and (c) mean C-rate.

Cars increases by 0.6 to 1.4 percentage points when FCR or intraday trading is performed (Figure 5 d)). For the e-Buses, the increase is 0.3 to 0.8 percentage points (Figure 5 e)). Most e-Boats also show only low rates of increase in mean SOC. Deviating from this, the mean SOC of one e-Boat (downward-pointing triangle) increases by 4 percentage points in FCR to 9 percentage points in arbitrage. This e-Boat has a mean plugged and idle time of 74.8% and can therefore often be used for V2X.

Figure 5 g) – i) present the mean C-rate of the vehicles in the paused charging and V2X strategies. In particular, the provision of FCR strongly reduces the mean C-rate experienced by the vehicle batteries. For example, the mean C-rate of the median e-Car decreases by 90% and of the median e-Bus by 46%. Providing intraday trading or PS also reduces the mean C-rates, but not as much as FCR. This is because FCR often demands low power values relative to the marketed power. In contrast, the power values provided in intraday trading and PS are higher. The fact that mean C-rates are reduced in all V2X markets shows that for the simulated pool sizes, the loads that vehicle batteries experience during V2X provision are often lower than the loads during typical driving and charging.

4.4 Exemplary degradation analysis of e-Car battery with and without V2X

In addition to quantifying parameters such as mean SOC or number of EFCs, *SimSES* can also be used to simulate the aging of vehicle batteries. As described in section 3.3, an LFP cell was simulated for this purpose over one year. The capacity losses of the e-Car batteries after one year range from 6.2% to 7.1% for all four strategies, mainly due to the calendric degradation caused by the high SOCs. Figure 6 shows the change in the capacity loss of the e-Car batteries when providing V2X services relative to the paused, unidirectional strategy over each e-Car's mean V2X-ready ratio. For example, if an e-Car has lost 500 Wh of its nominal capacity in a year in the paused strategy and 505 Wh in a V2X strategy, the relative change in capacity loss corresponds to 1%.

In general, the V2X provision increases the capacity loss for the simulated cell. PS has the least influence on aging due to only slightly higher cyclization at comparatively low powers (see Figure 5). In a few cases, such as one e-Car with a mean V2X-ready ratio of 77.3%, the utilization for PS seems to reduce aging compared to the paused charging strategy (-0.15%). In these cases, the vehicle encounters only slightly more EFCs when providing PS compared to the paused charging strategy,

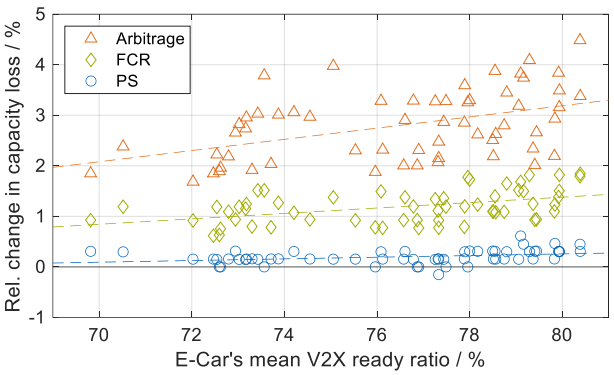

Fig. 1. Change in capacity loss of the e-Car batteries for the V2X strategies compared to the paused charging strategy without V2X over each e-Car's mean V2X-ready ratio. Each of the 60 e-Cars appears once in the diagram for each V2X strategy. The dashed lines show a linear fit for each V2X application across all cars. In the 1-year *SimSES* simulation, a Sony LFP battery with a degradation model from Naumann et al. is used [21,22].

which slightly increases cyclic battery aging. For the exemplary e-Car, the increase is 2.2 EFCs in the one-year simulation period. At the same time, providing PS decreases the mean SOC, reducing calendar aging (exemplary e-Car from 90.59% to 90.34%). The two effects subsequently overlap, which can reduce the total capacity loss of the battery despite the provision of PS in a few cases.

Providing FCR with the e-Cars results in a more significant loss of capacity in the simulations than providing PS. The aging is most severe if arbitrage trading is performed with the e-Cars. But even here, the maximum capacity loss increase compared to the paused charging strategy is 4.5%. This is because the LFP cell used is considered relatively cycle stable and can thus tolerate the increase in EFCs well.

Figure 6 also shows that e-Cars with higher mean V2X-ready ratios also lead to larger capacity loss increases due to V2X provision (dashed lines). This trend holds true for all three V2X applications. However, when individual cars are examined, it can be observed that a higher V2X-ready ratio does not always lead to a higher increase in capacity loss. This is because the mean value of the V2X-ready ratio is not the only factor of relevance, but also the times at which the car is available and the times of V2X demand. Whether the increase in capacity loss can be compensated by generated revenues on the electricity (arbitrage) and power (FCR) markets or by avoided grid charges (PS) depends on the current prices or costs of the respective location.

5. CONCLUSION AND OUTLOOK

In the present work, the V2X deployment of three means of transport was simulated and investigated. For this purpose, a dataset of 60 simulated e-Cars, 52 field-data e-Buses, and six field-data e-Boats was used on the one hand, and data from stationary BSS applications on the other. First, the vehicles were examined in terms of their predictability. It was found that in particular private e-Cars behave predictably at night. Furthermore, an analysis of idle times showed that V2X availability varies over the week, with e-Cars and e-Buses being mostly available at night. Another focus was the simulation of V2X provision in the simulation tool *SimSES*. This allowed battery-relevant parameters and the aging of the LIBs to be quantified. For example, the former showed that, compared to a paused charging strategy, the number of EFCs increases by 42% to 50% with FCR or intraday arbitrage for e-Cars and by 7% to 13% for e-Buses due to V2X deployment. The example aging simulation of the e-Car LIBs showed an increased capacity loss, especially for intraday arbitrage trading and FCR provision.

Building on the present work, further research areas can be identified. The results of section 4.3 and section 4.4 depend strongly on the pool composition and power allocation among the vehicles. Thus, pools could be formed from varying numbers of vehicles and from different vehicle types, such as a combination of e-Cars and e-Buses. Furthermore, in addition to the equal distribution of the required power to all available vehicles, a cascaded distribution or a distribution according to the remaining capacity of the batteries could also be implemented. Moreover, if the vehicles were actively discharged to 50% SOC, for example, the potential for V2X provision would increase, but the load on vehicle batteries would also rise. Additionally, more detailed analyses of battery aging could be made with further aging models and driving data over longer periods. Finally, the methodology and the results could also be used to evaluate the suitability of different battery cells for vehicles with and without V2X.

AUTHOR CONTRIBUTIONS

Benedikt Tepe: Conceptualization, Methodology, Software, Investigation, Writing - Original Draft, Visualization. **Sammy Jablonski:** Conceptualization, Methodology, Writing – Original Draft. **Anupam Parlikar:** Conceptualization, Methodology, Writing – Original Draft. **Holger Hesse:** Conceptualization, Writing - Review & Editing, Supervision. **Andreas Jossen:** Resources, Writing - Review & Editing, Supervision.

ACKNOWLEDGEMENT

This work was financially supported by the German Federal Ministry of Education and Research (BMBF) within the SimBAS project (Grant No. 03XP0338A), which is managed by Project Management Jülich. The responsibility for this publication rests with the authors.

DECLARATION OF INTEREST STATEMENT

The authors declare that they have no known competing financial interests or personal relationships that could have appeared to influence the work reported in this paper.

REFERENCE

[1] International Energy Agency. Global EV Outlook 2023: Catching up with climate ambitions. Paris; 2023.

[2] Bloomberg New Energy Finance. Electric Buses in Cities: Driving Towards Cleaner Air and Lower CO2. Bloomberg Finance LP 2018.

[3] Joshi S. Electric Boat Market Size Worth $11.35 Billion, Globally, by 2028 at 13.7% CAGR: The Insight Partners. GlobeNewswire 2022, 8 November 2022; Available from: https://www.globenewswire.com/en/news-release/2022/11/08/2551096/0/en/Electric-Boat-Market-Size-Worth-11-35-Billion-Globally-by-2028-at-13-7-CAGR-The-Insight-Partners.html. [August 18, 2023].

[4] Figgener J, Hecht C, Haberschusz D, Bors J, Spreuer KG, Kairies K-P et al. The development of battery storage systems in Germany: A market review (status 2023); 2023.

[5] Gschwendtner C, Sinsel SR, Stephan A. Vehicle-to-X (V2X) implementation: An overview of predominate trial configurations and technical, social and regulatory challenges. Renewable and Sustainable Energy Reviews 2021;145:110977. https://doi.org/10.1016/j.rser.2021.110977.

[6] Borge-Diez D, Icaza D, Açıkkalp E, Amaris H. Combined vehicle to building (V2B) and vehicle to home (V2H) strategy to increase electric vehicle market share. Energy 2021;237:121608. https://doi.org/10.1016/j.energy.2021.121608.

[7] Tepe B, Figgener J, Englberger S, Sauer DU, Jossen A, Hesse H. Optimal pool composition of commercial electric vehicles in V2G fleet operation of various electricity markets. Applied Energy 2022;308:118351. https://doi.org/10.1016/j.apenergy.2021.118351.

[8] Kempton W, Tomic J, Letendre S, Brooks A, Lipman T. Vehicle-to-grid power: battery, hybrid, and fuel cell vehicles as resources for distributed electric power in California 2001.

[9] Uddin K, Dubarry M, Glick MB. The viability of vehicle-to-grid operations from a battery technology and policy perspective. Energy Policy 2018;113:342–7. https://doi.org/10.1016/j.enpol.2017.11.015.

[10] Thingvad A, Calearo L, Andersen PB, Marinelli M. Empirical Capacity Measurements of Electric Vehicles Subject to Battery Degradation from V2G Services. IEEE Trans. Veh. Technol. 2021:1. https://doi.org/10.1109/TVT.2021.3093161.

[11] SimSES: Software for techno-economic simulation of stationary energy storage systems; 2017.

[12] Tepe B, Jablonski S, Hesse H, Jossen A. Lithium-ion battery utilization in various modes of e-transportation. eTransportation 2023:100274. https://doi.org/10.1016/j.etran.2023.100274.

[13] Tepe B, Jablonski S, Hesse H, Jossen A. Lithium-Ion Battery Utilization in various Modes of e-Transportation - Dataset. https://doi.org/10.14459/2023mp1709192.

[14] Kucevic D, Tepe B, Englberger S, Parlikar A, Mühlbauer M, Bohlen O et al. Standard battery energy storage system profiles: Analysis of various applications for stationary energy storage systems using a holistic simulation framework. Journal of Energy Storage 2020;28:101077. https://doi.org/10.1016/j.est.2019.101077.

[15] Collath N, Cornejo M, Engwerth V, Hesse H, Jossen A. Increasing the lifetime profitability of battery energy storage systems through aging aware operation. Applied Energy 2023;348:121531. https://doi.org/10.1016/j.apenergy.2023.121531.

[16] Gaete-Morales C, Kramer H, Schill W-P, Zerrahn A. An open tool for creating battery-electric vehicle time series from empirical data, emobpy. Sci Data 2021;8(1):152. https://doi.org/10.1038/s41597-021-00932-9.

[17] Möller M, Kucevic D, Collath N, Parlikar A, Dotzauer P, Tepe B et al. SimSES: A holistic simulation framework for modeling and analyzing stationary energy storage systems. Journal of Energy Storage 2022;49:103743. https://doi.org/10.1016/j.est.2021.103743.

[18] Arnold G, Brandl R, Degner T, Gerhardt N, Landau M, Nestle D et al. Intelligente Netzanbindung von Elektrofahrzeugen zur Erbringung von Systemdienstleistungen—INEES. Wolfsburg,

Hamburg, Niestetal, Kassel: Volkswagen AG, LichtBlick SE, SMA Technology AG, Fraunhofer IWES 2015.
[19] Collath N, Tepe B, Englberger S, Jossen A, Hesse H. Aging aware operation of lithium-ion battery energy storage systems: A review. Journal of Energy Storage 2022;55:105634. https://doi.org/10.1016/j.est.2022.105634.
[20] Han X, Lu L, Zheng Y, Feng X, Li Z, Li J et al. A review on the key issues of the lithium ion battery degradation among the whole life cycle. eTransportation 2019;1:100005. https://doi.org/10.1016/j.etran.2019.100005.
[21] Naumann M, Schimpe M, Keil P, Hesse H, Jossen A. Analysis and modeling of calendar aging of a commercial LiFePO4/graphite cell. Journal of Energy Storage 2018;17:153–69. https://doi.org/10.1016/j.est.2018.01.019.
[22] Naumann M, Spingler FB, Jossen A. Analysis and modeling of cycle aging of a commercial LiFePO4/graphite cell. Journal of Power Sources 2020;451:227666. https://doi.org/10.1016/j.jpowsour.2019.227666.
[23] Schmalstieg J, Käbitz S, Ecker M, Sauer DU. A holistic aging model for Li(NiMnCo)O2 based 18650 lithium-ion batteries. Journal of Power Sources 2014;257:325–34. https://doi.org/10.1016/j.jpowsour.2014.02.012.
[24] Bibra EM, Connelly E, Dhir S, Drtil M, Henriot P, Hwang I et al. Global EV Outlook 2022: Securing supplies for an electric future. International Energy Agency (IEA) 2022.
[25] Tepe B, Figgener J, Englberger S, Jossen A, Uwe Sauer D, Hesse H. Analysis of optimally composed EV pools for the aggregated provision of frequency containment reserve and energy arbitrage trading. In: 5th E-Mobility Power System Integration Symposium (EMOB 2021). Institution of Engineering and Technology; 2021, p. 175–180. https://doi.org/10.1049/icp.2021.2521.